ISDRS 2013, December 11-13. 2013

III-nitride Tunnel Injection Hot Electron Transfer Amplifier (THETA) with Common-emitter Gain

Digbijoy N. Nath[a], Zhichao Yang[a], Pil Sung Park[a] and Siddharth Rajan[a]

[a] *Department of Electrical Engineering, The Ohio State University, Columbus, USA.*

We report on the design and demonstration of the first III-nitride tunnel-injected hot electron amplifier transistor (THETA). Vertical devices are promising candidates for achieving high frequency operation due to their ability to engineer electron transport over very short distances. Unlike InP and SiGe HBT technologies, bipolar GaN devices are challenging due to poor hole ionization energy and difficulties in achieving high p-doping and ultra-low p-contact. In this work, we demonstrate tunnel injection vertical transistors based on III-nitrides with current transfer ratio >0.80.

A THETA [1] is based on tunnel-injecting electrons through an emitter barrier followed by ballistic transport to the collector through a thin base. A thin heavily doped base is desired to minimize electron relaxation and base sheet resistance. Hot electrons which do not relax in the base travel ballistically and are collected by a reverse biased collector. Detailed calculations for the III-nitride THETA will be described to show that cutoff frequencies >1 THz could be achieved in a GaN-based THETA by exploiting tunneling injection and ballistic transport.

The MBE-grown epitaxial stack consisted of 3.5 nm $Al_{0.3}Ga_{0.7}N$ emitter barrier, degenerately doped GaN base, a thin $In_{.15}Ga_{.85}N$ to induce an electrostatic base-collector barrier with 7 nm UID GaN and AlGaN graded from 20% to GaN as confirmed with XRD scan. We find random alloys based on AlGaN do not provide base/collector current blocking and adopted an approach using a polarization engineered non-random alloy barrier with significantly lower leakage. A base thickness series of 18, 9 and 6 nm will be presented. Al/Ni/Au/Ni emitter metallization, Cl_2-based ICP-RIE self-aligned base etch, Al/Ni/Au/Ni base contact, collector mesa etching and collector contact evaporation were done. The emitter area was 10 μm^2 and base mesa area was 100 μm^2.

The base-emitter I-V showed no temperature dependence indicating tunnel injection. Emitter current densities ~ 20-60 kA/cm^2 were observed (at 3 V bias). The base-collector leakage was <10 A/cm^2 at 1 V while the base-to-base I-V between two base pads of a device showed Ohmic behavior and low base sheet resistance (2-3 kΩ/□).

Devices exhibited output modulation (I_C-V_{CE}) in common emitter configuration (emitter at ground). Output current I_C was observed to increase as the input bias V_{BE} was increased. The Gummel plot showing collector current as a function of emitter bias at zero base collector shows that large fraction of injected electrons travel ballistically to the collector. Shrinking the base thickness in the three samples was found to increase the current transfer ratio ‘α’, and a maximum α ~ 0.82 at 6 V base-emitter bias was measured for sample with 6 nm base thickness. The parasitic voltage drop in the base-access region due to high base resistance was found to limit the transfer ratio dependence on base-emitter bias.

In conclusion, we show the design and demonstration of the first vertical tunneling based unipolar III-nitride devices with low leakage, high current gain, and ballistic transport with potential to terahertz electronics. This work is funded by Office of Naval Research under the DATE MURI project (Program manager: Dr. Paul Maki).

References

[1] Mordehai Heiblum, "Tunneling hot electron transfer amplifiers (THETA): Amplifiers operating up to the infrared." *Solid-State Electronics* 24.4, 343-366, (1981).

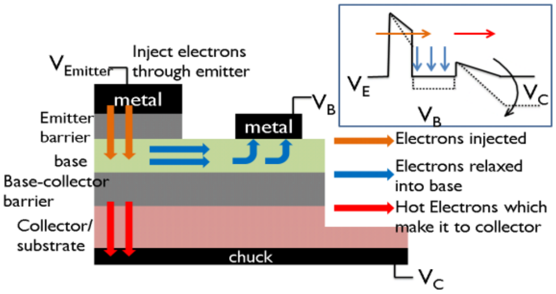

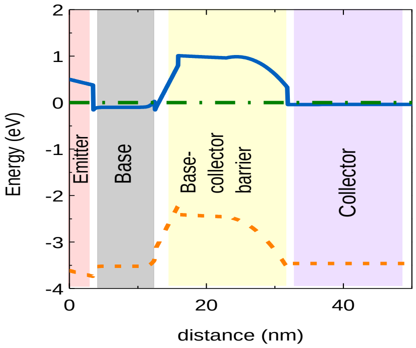

Fig. 1: Schematic of THETA & its operational procedure. Inset: schematic of band-diagram of device in operation

Fig.2: Energy-band diagram of THETA

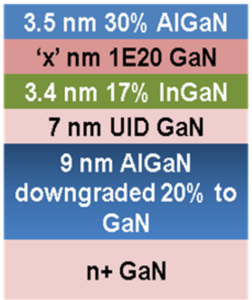

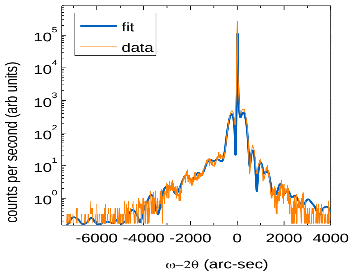

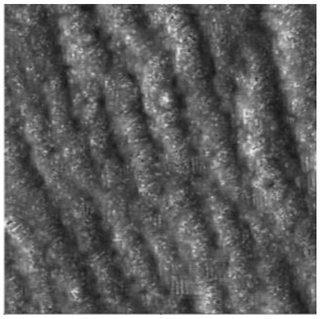

Fig. 3: Epitaxial stack (THETA)

Fig. 4: HRXRD ω-2θ scan with fitting

5: AFM scan (5x5 um; data scale = 3.5 nm)

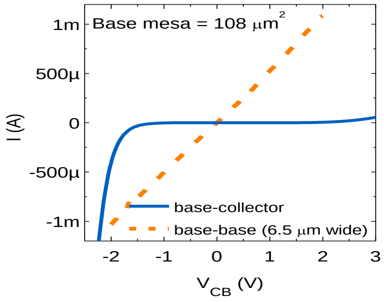

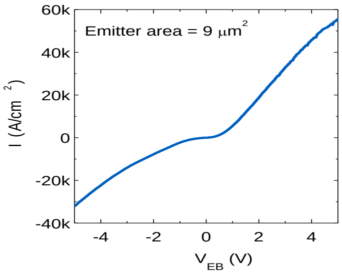

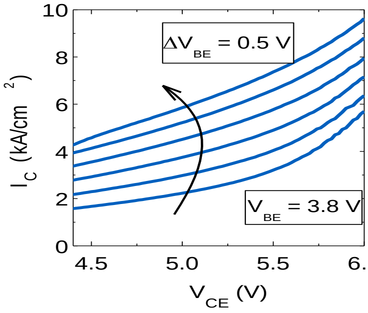

Fig. 6: Base-collector I-V (very low leakage)

Fig. 7: Base-emitter I-V

Fig 8: Output characteristics common-emitter

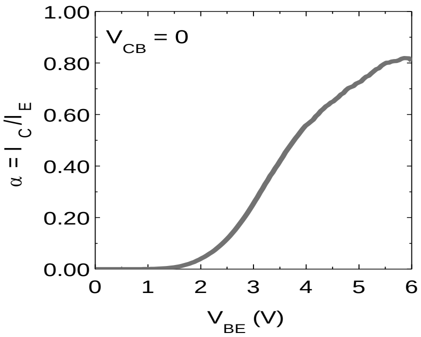

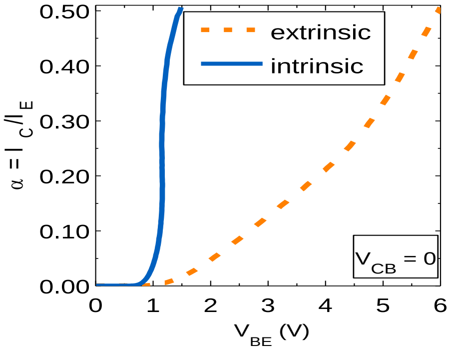

Fig 9: Current transfer ratio (sample with 6 nm base)

Fig 10: Transfer ratio dependence on extrinsic and intrinsic base-emitter bias